Mechanisms of gold biomineralization in the bacterium *Cupriavidus metallidurans*

Frank Reith[a,b,1], Barbara Etschmann[c,d,e], Cornelia Grosse[f], Hugo Moors[g], Mohammed A. Benotmane[g], Pieter Monsieurs[g], Gregor Grass[h], Christian Doonan[i], Stefan Vogt[j], Barry Lai[j], Gema Martinez-Criado[k], Graham N. George[l], Dietrich H. Nies[f], Max Mergeay[g], Allan Pring[c], Gordon Southam[m], and Joël Brugger[a,c]

[a]Centre for Tectonics, Resources and Exploration, School of Earth and Environmental Sciences, University of Adelaide, North Terrace, SA 5000, Australia; [b]Environmental Biogeochemistry, Commonwealth Scientific and Industrial Research Organisation (CSIRO) Land and Water, PMB2, Glen Osmond, SA5064, Australia; [c]Department of Mineralogy, South Australian Museum, Adelaide, SA 5005, Australia; [d]CSIRO Exploration and Mining, c/o Mineralogy, South Australian Museum, Adelaide, SA 5000, Australia; [e]CODES Centre of Excellence, University of Tasmania, TAS 7001 Hobart, Australia; [f]Martin-Luther-Universität Halle-Wittenberg, Institut für Biologie/Mikrobiologie, DE-06120 Halle, Germany; [g]Expertise Group for Molecular and Cellular Biology, Unit for Microbiology, Nuclear Research Centre, Institute for Environment, Health and Safety, Boeretang 200, B-2400 MOL, Belgium; [h]School of Biological Sciences, University of Nebraska-Lincoln, Lincoln NE 68588-0666 ; [i]Department of Chemistry and Biochemistry, University of California, Los Angeles, CA 90095-1569; [j]Advanced Photon Source, Argonne National Laboratory, Argonne, IL 60439; [k]Experiments Division, European Synchrotron Radiation Facility, 38043-Grenoble, France; [l]Department of Geological Sciences, University of Saskatchewan, 114 Science Place, Saskatoon, S7N 5E2, Canada; and [m]Department of Earth Sciences/Department of Biology, University of Western Ontario, London, ON, Canada N6A 5B7

Edited by Douglas C. Rees, California Institute of Technology, Pasadena, CA, and approved August 27, 2009 (received for review April 29, 2009)

While the role of microorganisms as main drivers of metal mobility and mineral formation under Earth surface conditions is now widely accepted, the formation of secondary gold (Au) is commonly attributed to abiotic processes. Here we report that the biomineralization of Au nanoparticles in the metallophillic bacterium *Cupriavidus metallidurans* CH34 is the result of Au-regulated gene expression leading to the energy-dependent reductive precipitation of toxic Au(III)-complexes. *C. metallidurans*, which forms biofilms on Au grains, rapidly accumulates Au(III)-complexes from solution. Bulk and microbeam synchrotron X-ray analyses revealed that cellular Au accumulation is coupled to the formation of Au(I)-S complexes. This process promotes Au toxicity and *C. metallidurans* reacts by inducing oxidative stress and metal resistances gene clusters (including a Au-specific operon) to promote cellular defense. As a result, Au detoxification is mediated by a combination of efflux, reduction, and possibly methylation of Au-complexes, leading to the formation of Au(I)-C-compounds and nanoparticulate Au^0. Similar particles were observed in bacterial biofilms on Au grains, suggesting that bacteria actively contribute to the formation of Au grains in surface environments. The recognition of specific genetic responses to Au opens the way for the development of bioexploration and bioprocessing tools.

bacteria | XAS

Microorganisms are paramount for metal cycling and mineral formation in Earth surface environments (1–3). Metal cycles are driven by microorganisms, because some metal ions are essential for microbial nutrition, others are oxidized or reduced to obtain metabolic energy, while in particular heavy metal ions, e.g., Hg^{2+}, Cd^{2+}, Ag^{+}, Co^{2+}, CrO_4^{2}, Cu^{2+}, Ni^{2+}, Pb^{2+}, Zn^{2+}, also cause toxic effects (4). To counter these effects, microorganisms have developed genetic and proteomic responses to strictly regulate metal homeostasis (5). Metallophilic bacteria, such as the Gram-negative β-proteobacterium *Cupriavidus metallidurans*, harbor numerous metal resistance gene clusters enabling cell detoxification via a number of mechanisms such as complexation, efflux, or reductive precipitation (6). Hence metallophillic bacteria thrive in environments containing high concentrations of mobile heavy metal ions, such as mine waste rock piles, efflux streams of metal processing plants, and naturally mineralized zones (6).

In contrast to most other metals, gold (Au) is rare, inert, nonessential, and does not form free ions in aqueous solution under surface conditions (4). Therefore, the role of microorganisms in the environmental cycling of Au, i.e., its solubilization, dispersion, and reconcentration, remains controversial; most authors emphasize abiogenic pathways (7, 8), some argue for a passive role of microorganisms in promoting Au mobility (9, 10), and others advocate an active role of microorganism in the formation of "bacterioform" Au and secondary Au grains (4, 11). Similar to free metal ions, Au-complexes appear to be toxic to bacteria, because once inside the cell, they may generate oxidative stress and inhibit enzyme function (5). An Au-specific efflux system regulated by a MerR-like transcriptional activator (GolS), a putative efflux P-type ATPase (GolT), and metallochaperone (GolB) regulates cytoplasmic Au concentrations in the enterobacterium *Salmonella enterica*; however, the formation of particulate Au was not observed (12). Biofilms dominated by *C. metallidurans* are common on Au grains retrieved from soils and sediments from temperate and tropical Australian sites (13). Amendment of *C. metallidurans* with Au(III)-hydroxychloride complexes led to the concentration of Au in discrete areas in some cells, while Au was distributed homogenously throughout other cells (13). This duality suggests that *C. metallidurans* scavenges Au(III) via a two-stage mechanism, which may have evolved as specific ways for survival in Au-rich environments, where Au-detoxification biominerals may be formed.

To understand the fundamental mechanisms of Au biomineralization and the impact of microbial processes on Au mobility in environmental systems, the effect of indigenous bacteria such as *C. metallidurans* on Au-complexes as well as their cellular responses to these complexes need to be understood. In this study we addressed the following questions: (i) Is the reduction of Au(III)-complexes in *C. metallidurans* an active, energy-dependent process, a passive sorption mechanism, or a combination of both? (*ii*) How is the Au distributed and speciated in the cells, and in which form is Au present in biofilms on Au grains? (*iii*) What are the genetic/biochemical responses to the presence of Au complexes in *C. metallidurans*? Finally, we discuss how integrated studies combining synchrotron microanalysis, geochemistry, and (meta)-genomics will transform our understanding of metal cycling in the environment, and lead to applications in mineral exploration and bioprocessing.

Results

Au(III) Accumulation by *C. metallidurans*: Effect of Metabolic State and Solution pH. The metabolic state of cells and solution pH had a marked effect on the accumulation of Au(III) by *C. metallidurans*.

Author contributions: F.R., C.G., G.G., and J.B. designed research; F.R., B.E., C.G., H.M., C.D., A.P., G.S., and J.B. performed research; M.A.B., S.V., B.L., G.M.-C., G.N.G., D.H.N., G.S., and J.B. contributed new reagents/analytic tools; F.R., B.E., C.G., H.M., P.M., C.D., D.H.N., M.M., A.P., and J.B. analyzed data; and F.R. wrote the paper.

The authors declare no conflict of interest.

This article is a PNAS Direct Submission.

[1]To whom correspondence should be addressed. E-mail: frank.reith@csiro.au.

This article contains supporting information online at www.pnas.org/cgi/content/full/0904583106/DCSupplemental.

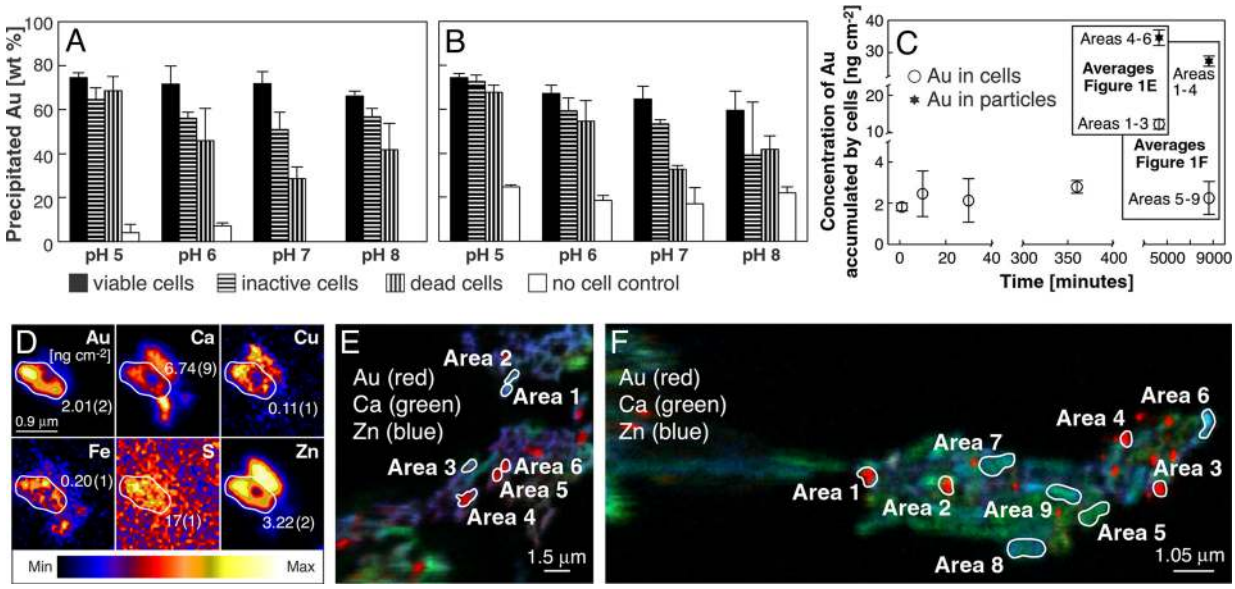

Fig. 1. Accumulation of Au(III)-complexes by *C. metallidurans*. (*A* and *B*) Concentration of Au(III) taken up after 6 h (*A*) and 144 h (*B*) of incubation; cells were incubated in PME-medium at starting pHs 5.0, 6.0, 7.0, and 8.0 and amended with 50 μM Au(III); error bars represent the standard deviation of triplicate samples; (*C*) concentrations of Au in individual *C. metallidurans* cells and particles associated with cells in [ng cm^{-2}] based on quantitative μXRF maps, error bars represent the standard deviation of replicate samples; (*D*) quantitative μXRF-maps showing the distribution of Au, Ca, Cu, Fe, S, and Zn in an individual cell after 1 min exposure to Au(III) at pH 7.0 [the quantified area is marked in the image, and concentrations ($\pm$ calculated errors) are given in the image, concentration ranges for elements are Au, 0–4.16; Ca, 0–18.78; Cu, 0–0.29; Fe, 0–0.44; S, 0–60.52; and Zn, 0–24.57 ng cm^{-2}]; (*E* and *F*) overlay false color quantitative μXRF-maps of the distribution of Au (red), Zn (blue), and Ca (green) in cell clusters after 72 h (*E*) and 144 h (*F*) of incubation at pH 7.0.

Under all metabolic conditions tested, the concentration of Au(III) accumulated by the cells was lower at higher starting pHs (Fig. 1 *A* and *B* and *SI Materials and Methods*). In experiments with inactive and dead cells, no significant pH changes occurred during the 144-h incubation period, and uptake of Au was similar after 6 and 144 h (Fig. 1 *A* and *B*), suggesting pH dependency of the initial Au sorption. This was also observed by other authors, who showed that at lower pHs, cell wall ligands are protonated to a higher degree, resulting in an overall more positive surface charge, which increases the electrostatically driven passive sorption of the negatively charged Au(III)-complex onto the cells (14, 15). Metabolically active cells accumulated the highest amounts of Au(III) under all starting pH conditions, i.e., between 74.6 wt% (pH 5.0) to 66.2 wt% (pH 8.0) of Au(III) after 6 h (Fig. 1*A* and *SI Materials and Methods*). At starting pH 7.0, the highest numbers of viable cells and largest difference in uptake between active and inactive/dead cells were detected (Fig. 1*A* and Fig. S1*A*). After 144 h, the total concentration of Au taken up by metabolically active cells had changed little, and the final pH approximated 7.0 irrespective of starting pH (*SI Materials and Methods* and Fig. 1*B*). Purple precipitates appeared in cultures containing metabolically active cells, suggesting formation of 100-nm-sized colloidal Au^0 (16). In contrast, in metabolically inactive and dead cell experiments, no precipitate was observed (*SI Materials and Methods*). These results indicate that metabolic activity increases the capacity of cells to take up Au and controls its reduction to Au^0, which follows the initial pH-dependent accumulation that is the result of passive sorption.

Au(III) Accumulation by *C. metallidurans*: Uptake Kinetics and Distribution. Kinetic experiments with metabolically active cells [incubated with 50 μM Au(III), 1 min to 144 h, pH 7.0] confirmed a two-stage reduction for Au(III)-complexes (Fig. 1 *C–F* and *SI Materials and Methods*). The distribution of Au and other elements (i.e., S, Ca, Fe, Cu, Zn, Mn; Fig. 1*D* and Figs. S2–S5) was mapped in individual cells using synchrotron μ-X-ray fluorescence (μXRF) (Fig. 1 *C–F* and Figs. S2–S5). A spot size of 120 × 150 nm enabled the collection of over 30 spectra per cell. Heavier elements expected in bacterial cells (Fig. 1*D*, *SI Materials and Methods*, and Figs. S2–S5) were successfully mapped. Calcium, Zn, and Cu, which can make up to 0.5 wt%, 0.03 wt%, and 0.005 wt% of the dry weight of bacterial cells, respectively (17), are shown in overlays with Au to assess the location of Au associated with cells (Fig. 1 *E* and *F* and Figs. S2 and S3). Copper and Zn were dispersed throughout the cells Ca was mostly detected in cell envelopes, presumably due to its function as stabilizer of cell membranes (Fig. 1 *E* and *F* and Figs. S2 and S3) (18). After 1 min of exposure to Au(III), cells had taken up 1.82 $\pm$ 0.19 ng cm^{-2} of Au, and accumulated Au was distributed throughout the cells (Fig. 1 *C* and *D*). The concentrations of accumulated Au in cells increased to 2.79 $\pm$ 0.31 ng cm^{-2} after 6 h and to 12.2 $\pm$ 1.3 ng cm^{-2} after 72 h (Fig. 1*C*). After 72 h, zones containing up to 34.6 $\pm$ 2.4 ng cm^{-2} Au were detected (Fig. 1 *C* and *E* and Fig. S4). These "hot spots" were associated with cell envelopes and had not been observed earlier. After 144 h of exposure, Au concentrations in the cytoplasm decreased to 2.25 $\pm$ 0.79 ng cm^{-2}; in contrast, regions of the cell envelope containing high Au concentrations were more numerous and larger (Fig. 1 *C* and *F* and Fig. S5). This suggests that cells actively removed Au from the cytoplasm and precipitated it as nanoparticulate Au^0 in the periplasm, as confirmed by transmission electron microscope (TEM) (Fig. 2*A* and *SI Materials and Methods*); particulate Au was also present in the cytoplasm suggesting cytoplasmic reduction (Fig. S6). This suggests that a combination of several mechanisms may be used by *C. metallidurans* to detoxify Au(III)-complexes and points to energy-dependent efflux as well as intra- and extracellular reductive precipitation.

Speciation of Au in *C. metallidurans*. X-ray absorption near edge structure (XANES) spectra collected from cell pellets after 6 h of exposure to Au(III)-complexes showed that 100 wt% of the accumulated Au was converted to a Au(I)-S species (Fig. 3 and *SI Materials and Methods*), as was observed in cyanobacteria (19). Linear combination fitting (LCF) of spectra collected after 72 h to model spectra showed that 53.0 wt% of Au were present as Au(I)-S, 28.7 wt% as metallic Au^0, and 18.3 wt% as Au(I)-C (Fig. 3*A*). To

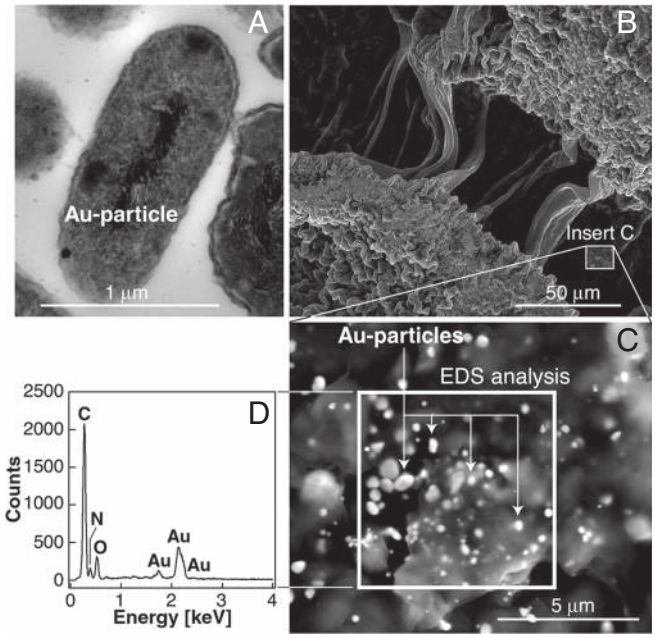

Fig. 2. Transmission electron micrograph (TEM) of a *C. metallidurans* ultra-thin section containing a Au nanoparticle in the periplasmic space (*A*). Scanning electron microscopy micrographs (*B* and *C*) with energy dispersive X-ray analysis (SEM-EDXA) (*D*) of a biofilm containing particulate Au (*C*) growing on a Au grain from the Prophet Gold Mine, Australia.

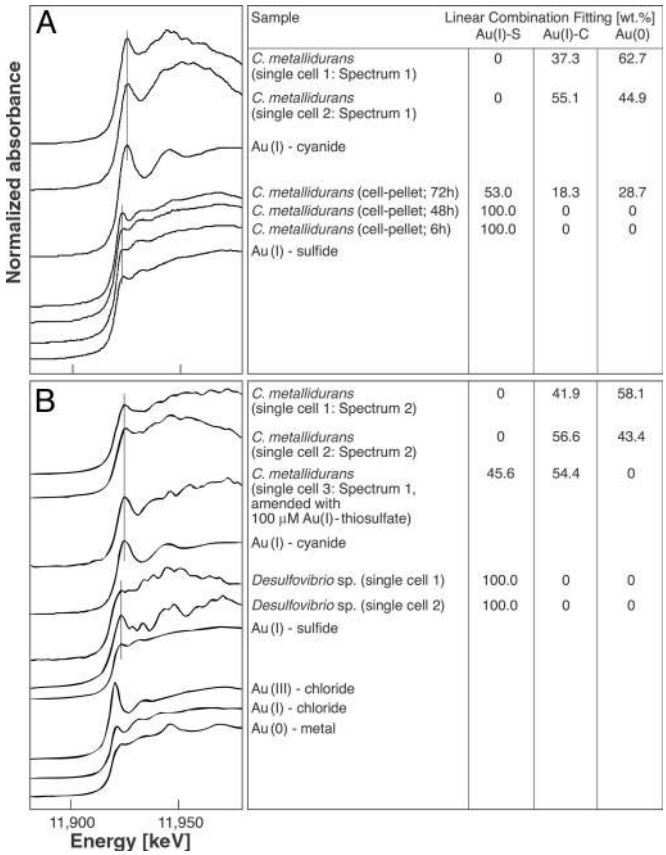

Sample	Linear Combination Fitting [wt.%] Au(I)-S	Au(I)-C	Au(0)
C. metallidurans (single cell 1: Spectrum 1)	0	37.3	62.7
C. metallidurans (single cell 2: Spectrum 1)	0	55.1	44.9
Au (I) - cyanide			
C. metallidurans (cell-pellet; 72h)	53.0	18.3	28.7
C. metallidurans (cell-pellet; 48h)	100.0	0	0
C. metallidurans (cell-pellet; 6h)	100.0	0	0
Au (I) - sulfide			
C. metallidurans (single cell 1: Spectrum 2)	0	41.9	58.1
C. metallidurans (single cell 2: Spectrum 2)	0	56.6	43.4
C. metallidurans (single cell 3: Spectrum 1, amended with 100 μM Au(I)-thiosulfate)	45.6	54.4	0
Au (I) - cyanide			
Desulfovibrio sp. (single cell 1)	100.0	0	0
Desulfovibrio sp. (single cell 2)	100.0	0	0
Au (I) - sulfide			
Au (III) - chloride			
Au (I) - chloride			
Au (0) - metal			

Fig. 3. (*A*) XANES spectra and results of LCF of Au in *C. metallidurans* cell pellets (after 6, 48, and 72 h; amended with 50 μM Au(III), individual *C. metallidurans* cells [after144 h; amended with 100 μM Au(III)]. (*B*) XANES spectra and results of LCF of Au in individual *C. metallidurans* cells [second spectrum on the same cells as shown in panel *A*, spectrum of 100 μM Au(I)-thiosulfate after144 h] and individual *Desulfovibrio* sp. cells amended with Au(I)-thiosulfate. Au-model substances in (*B*) are metallic Au, Au(I)-cyanide, Au(III)-chloride, Au(I)-chloride, and Au(I)-sulfide.

examine these results on the level of individual cells, μXANES spectra were obtained from individual cells after 6 days of incubation with Au(III). Peak fitting analyses showed that the initial Au(I)-S complex had disappeared and that the model compound that closely matched the obtained spectra is Au(I)-CN (Fig. 3*A*). LCF suggested the presence of 37.3 to 55.1 wt% of C-bound Au, the remainder being Au^0 (Fig. 3). To ensure that damage from the X-ray microbeam had not led to changes in Au speciation [e.g., reduction of Au(I)-S to metallic Au] during the collection of the first μXANES spectra, i.e., to ensure that the formation of Au(0) and Au(I)-C occurred as a result of biochemical reactions, three additional experiments were conducted (*SI Materials and Methods*): (i) A second μXANES spectrum was collected from the same spot, i.e., *C. metallidurans* cell, used to collect the first spectrum (Fig. 3 *A* and *B*). The second spectrum was similar to the first, and proportions of Au(0) and Au(I)-C had not changed significantly, indicating that the initial spectrum was not the result of beam damage (Fig. 3*B*). (*ii*) A spectrum was collected from a single *C. metallidurans* cell incubated with 100 μM Au(I)-thiosulfate, as a model for Au(I)-S, for 6 days under otherwise identical conditions (*SI Materials and Methods* and Fig. 3*B*). No metallic Au was present in these cells, demonstrating that metallic Au detected in Au(III) amended cells did not occur as a result of interaction of the X-ray beam with intermediate Au(I)-S-complex. (iii) A spectrum collected from *Desulfovibrio* sp. cells amended with Au(I)-thiosulfate (20) showed the typical Au(I)-S-signature with no metallic Au^0 or Au(I)-C, demonstrating that Au(I)-C and Au(I)-S spectra were well differentiated (Fig. 3*B*). Thus, the results demonstrate that Au(I)-C and Au^0 detected in *C. metallidurans* cells are the product of biochemical reactions and suggest that Au(III) was reduced to a Au(I)-S complex upon contact with *C. metallidurans*, which was taken up by the cells, and further reduced to Au^0. This points to detoxification via a reductive precipitation mechanism. Remarkably, a Au(I)-C-complex was generated, suggesting that *C. metallidurans* might use methylation of Au as an additional detoxification mechanism. Methylation of metals, e.g., Hg, Bi, Tn, or Ge, can be effected by microorganisms (21, 22) and has been proposed for Au (11). Methyl-Au contains a Au(I)-C bond (23), and its XANES spectrum is likely to be similar to that of the Au(I)-CN model compound.

Effect of and Response to Au(III)-Complexes on *C. metallidurans*. Minimal inhibitory concentration (MIC) of Au(III) for *C. metallidurans* CH34 in Tris-buffered mineral medium (TrisMM) is 2.0 μM for growth on solid media. In contrast, viable cells were detected in TrisMM and peptone meat extract (PME) media after amendment with up to 100 μM of Au(III) (*SI Materials and Methods* and Table S1). Thus, four microarray experiments were conducted to assess the cellular response to low (10 μM), medium (50 μM), and high (100 μM) concentrations Au(III) and different induction times (10 and 30 min; *SI Materials and Methods*) to induce Au stress, but not kill challenged cells. Circular plots reveal that upregulated as well as downregulated regions occurred on both chromosomes and plasmids (Fig. S7). At the threshold of 2-fold upregulation, 52 to 303 transcripts were up, and 32 to 229 of 6,205 transcripts were downregulated (Table S2). Expression of individual genes as well as overall expression increased consistently with increasing Au(III) concentrations [2.9-, 4.6-, and 6.1-fold after 10 min with 10, 50, and 100 μM Au(III), respectively], demonstrating concentration dependency of gene expression (*SI Materials and Methods* and Table S2). After 30 min with 50 μM Au(III), the highest individual transcription (137-fold in Rmet_4685) and an average 7.2-fold upregulation was observed, suggesting time de-

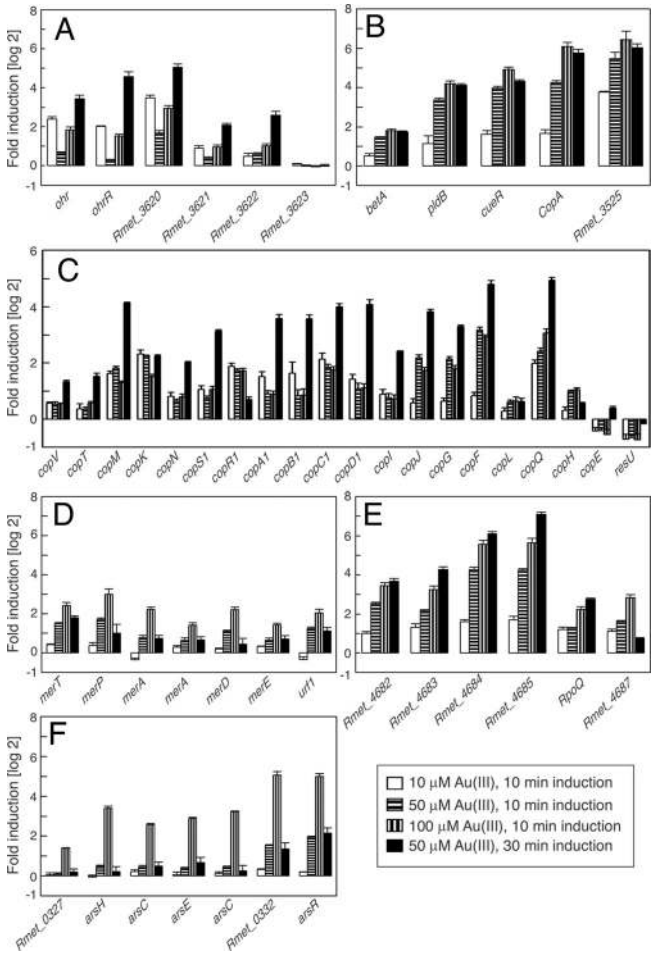

Fig. 4. Induction of metal resistance gene clusters in responsive to Au(III) toxicity at four different experimental conditions in *C. metallidurans* CH34. (*A*) *ohr*-cluster; (*B*) *cup*-cluster; (*C*) *cop*-cluster; (*D*) *mer*-cluster; (*E*) Au-specific Rmet_4682–4687 cluster; (*F*) *ars*-cluster.

pendency of Au-dependent gene regulation (Table S2). These results concord with the results of the μXRF mapping and suggest an active biochemical response of *C. metallidurans* to Au-stress.

The gene cluster Rmet_3618–3623 was upregulated under all conditions tested (Fig. 4*A*). This cluster comprises the *ohr* gene that confers resistance to H_2O_2-induced oxidative stress (24). Several other genes conferring oxidative stress resistance (e.g., *oxyR*, *ahpC*, *katA*, and *sodB*) were also upregulated (Table S2). This shows that one major toxic effect of Au(III) on *C. metallidurans* is the induction of oxidative stress. Expression of upregulated metal resistance clusters (i.e., *cup*, *cop*, *mer*, *ars*) occurred by stepwise induction and was proportional to Au(III) concentrations (Fig. 4 *B–D* and *F*). The *cup*/*cop* regions on chromosome 1 (*cupCAR*, Rmet_3525–3528) and on plasmid pMOL30 (*copVTMKNSRABC-DIJGFLQHE*, RALMEp20246–20239-RALMEp20236–20226) were strongly upregulated under all conditions tested (Fig. 4 *B* and *C*). The *cup*/*cop* clusters contain genes encoding for sensor-, chaperone-, efflux-, cytochrome C-, and oxido-reductase proteins regulating the cyto- and periplasmic detoxification of Cu(I/II) (25). The DNA-binding transcriptional activator CupR (Rmet_3525), an ortholog of CueR in *Escherichia coli* and GolS in *S. enterica*, the Cu-transporting P-type ATPase CopA, as well as CopI, and the putative electron transferring cytochrome C-type *copJ* were strongly upregulated, suggesting their involvement in efflux and reduction of Au(III/I) to Au(0) (12, 26, 27). Experiments with *C. metallidurans* had demonstrated the induction of *cupR* with Au(I)-complexes and suggested that a main function of CupR may be to defend *C. metallidurans* from Au-stress (27). Other metal ions, i.e., Ni^{2+}, Zn^{2+}, Cd^{2+}, Pb^{2+}, Hg^{2+}, Co^{2+}, have been shown to upregulate *cup*/*cop* genes (28). This suggests that the *cup*/*cop* system is a general metal response system that is readily inducible at low levels of metal stress, rather than a Cu-specific resistance system. The *mer* cluster, known to confer Hg resistance (6), was upregulated at concentrations of 50 and 100 μM Au(III) (Fig. 4*D*), suggesting cross-regulation of the Hg system by Au(III). This is possibly due to a physicochemical similarity of both elements (29). Additionally, a genomic region (Rmet_4682–4687) was highly (up to 137-fold) upregulated by the Au(III)-complexes (Fig. 4*E*), but not with other metals, suggesting the presence of a Au specific detoxification system. These results demonstrate that active biochemical detoxification occurred after challenging *C. metallidurans* with Au(III), and suggest that several detoxification mechanisms are used, whose induction is linked to the concentration of Au(III) in solution and the duration of exposure. Both Au-C and Au-S bonds are inferred from XANES spectroscopy (Fig. 3) and may be linked to Au toxicity responses. A number of Cup/Cop proteins contain putative metal ligand residues such as cysteine (CupR, CopG) and methionine (e.g., CopKABCIJ), which might form thiolates- or thioether-complexes with Au, respectively, as observed as Au(I)-S complexes by XANES (Fig. 3) (26). In addition, a number of methyltransferase genes (Rmet_0529, 3846, 4140), were upregulated with Au(III) but not with other metals tested (Table S2) (28), and the C-bound Au observed at 100 μM Au(III) may have been the result of Au-methylation.

Discussion

Biomineralization of Au in *C. metallidurans*. Reduction of Au(III)-complexes to Au^0-particles occurred via fast accumulation leading to the formation of intermediate Au(I)-S complexes, which was followed by a slow biochemically-driven reduction and intra- and extracellular deposition of metallic Au particles. This is consistent with the current understanding of aqueous Au chemistry (30): Upon sorption of Au(III) to cell surfaces, reduction to Au(I) occurred rapidly as a result of the high redox potential of Au(III)-complexes [e.g., E_0 = 1.002 V for the reaction $AuCl_4^- + 3\ e^- = Au(s) + 4\ Cl^-$]. This led to a "grab" of electrons from suitable electron donors, resulting in the induction of oxidative stress in cells, which reacted by upregulating oxidative stress response genes (Fig. 4*A*). The resulting Au(I)-complexes readily associate with nonpolar soft bases such as S, which are present in membrane and periplasmic proteins and led to the formation of the observed Au(I)-S species (Fig. 3*A*). Similar results were obtained in a XAS study assessing Au(III) reduction in the cyanobacterium *Plectonema boryanum*; here the reduction of Au(III)-complex to metallic Au involved the rapid (<2 min) formation of an intermediate Au(I)-S species and a slower reductive active pathway to Au^0 (19). The formation of intermediate Au(I)-S species was also observed in living and dead plant and microbial biomass amended with Au(III), suggesting that this may be general mechanism of passive Au accumulation (31, 32). However, reductase activity also led to the reduction of Au(III) to Au(I)-S-complex in bacteria (33), and based on our results, an active reduction cannot be ruled out as several upregulated genes show reductase function, e.g., CopI and MerA (Table S2). Active mechanisms are likely to be responsible for the slow reduction of Au(I)-S to metallic Au^0 particles. Similar to our study, Au particles in the cyanobacterial experiments were produced after Au(III) had been consumed by reaction with the culture (19). Accumulation and deposition of nanoparticles in *C. metallidurans* were observed after amendment with Ag(I)-thiosulfate, which led to the formation of membrane associated Ag particles (34).

The whole transcriptome analysis showed that upregulation of multiple metal resistance clusters depended on concentration and duration of the Au(III) challenge. Another study showed that multiple-metal responses by genes belonging to the *cop*, *cnr*, *mer*,

and *pbr* loci occurred after challenging *C. metallidurans* CH34 with Cd^{2+}, Pb^{2+}, Zn^{2+}, and Cu^{2+} (28). This suggests that *C. metallidurans* uses several strategies to reduce the intracellular concentration of toxic metal ions. In contrast, a study on Ag(I)-resistance in *C. metallidurans* and gene fusion studies found that responses were more specific toward the individual metal (34–36). This apparent contradiction may mainly reflect the differences in the timing of the responses to metal induction; 10 and 30 min for microarray, and up to several hours for gene fusions experiments. The present study also showed a higher degree of upregulation occurred in Rmet_4682 to Rmet_4687 after 30 min compared to the 10-min exposure (Fig. 4*E* and Table S2). This suggests that multiple-metal responses are transient early stages in resistance to heavy metals, which are followed by substrate-specific responses.

Au-dependent and Au-specific regulation occurs in bacteria despite Au being a rare, inert, and nonessential metal. A study with *E. coli* demonstrated the nonspecific regulation of transcription by Au(III)-complexes; CueR, an MerR-like transcriptional activator that usually responds to Cu(II), was also activated by Au(III), and this activation was promoted by binding of Au to the cysteine (Cys) residues 112 and 120 (26). In *C. metallidurans* the Cys residues 112 and 120 also play a key role in the specific binding of Au(I)-complexes to the transcriptional activator CupR, which is involved in the defense against Au stress (27). In another recent study Checa et al. (2007) characterized a transcriptional regulator (GolS) in *S. enterica*, which regulates the transcription of factors that endow *S. enterica* with resistance to Au(III) (12, 37). Expression of genes that were activated by GolS were described, the transmembrane efflux ATPase (GolT) and a metallochaperone (GolB) (12). A further GolS-regulated locus *gesABC* (for GolS-induced CBA efflux system-coding operon) was described recently; *gesABC* is a *Salmonella*-specific CBA efflux-system required for Au resistance in this bacterium (37). While Rmet_4682 to Rmet_4687 are not related to the GolSBT and GesABC systems, they appear to be of similar importance for *C. metallidurans* CH34, because of their strong induction with Au(III) (Fig. 4*E*). Rmet_4682–4687 is a divergon, encoding in one direction for an extracytoplasmic function (ECF) sigma factor (RpoQ = Rmet_4286) and its putative anti-sigma factor (Rmet_4287), which are transcribed as an operon (38). The sigma factor RpoQ belongs to a group with ECF (39), and the *rpoQ* gene was not induced by other metals in a transcriptome microarray study [e.g., 0.1 mM Cu(II)] (28); however, induction was shown for 0.3 mM Cu(II) using quantitative real-time RT-PCR (38). BLAST analyses of Rmet_4682 to Rmet_4685 conveyed little information about the function of these genes, other than they encode predicted membrane and transmembrane proteins. Because RpoQ may be required for expression of the Rmet_4285–4282 genes, we compared induction of the genes in this region for *C. metallidurans* CH34 (wild-type) and its Δ*rpoQ* (DN482) deletion mutant using quantitative RT-PCR (*SI Materials and Methods*) (38). In agreement with the microarray experiments, RT-PCR analysis showed that the transcription of Rmet_4285–4282, *rpoQ*, and Rmet_4687 was upregulated by Au(III) compared to no Au(III)-controls in *C. metallidurans* CH34. No difference in regulation between Au(III)-amended cells and no Au controls were observed in the *rpoQ* deletion mutant, indicating loss of transcription control of the genes Rmet_4285–4282. This demonstrates that the gene cluster Rmet_4285–4282 forms an operon, which is under control of the ECF sigma factor RpoQ, and that this sigma factor confers the Au response.

Implications for the Cycling of Au in Surface Environments. While this study shows that *C. metallidurans* harbors the potential to contribute to a biochemically driven biomineralization of Au in the environment, and the presence of *C. metallidurans* on secondary Au grains has to be established (13), field evidence for a microbial contribution to growth of secondary Au in the environment is necessary. Hence, to assess if nanoparticulate Au occurs in bacterial biofilms on Au grains, surface features of Au grains from Queensland, Australia, were studied using SEM-EDXA (Fig. 2 *B–D* and *SI Materials and Methods*). On eight of 10 grains, microbial biofilms composed of C, N, and O were observed (Fig. 2 *B* and *D*). Associated with the biofilms was nanoparticulate Au resembling Au-particles detected in *C. metallidurans* (Fig. 2*A*). This shows that Au biomineralization analogous to our experiments occurs in nature and provides strong evidence for an active contribution of microbiota the cycling of Au in the environment.

This research may explain some of the fundamental problems of secondary Au formation in surface environments that cannot be explained by the commonly accepted detrital model (4). According to this model, secondary Au grains in surface environments are primary in origin, i.e., formed in hydrothermal systems at high pressures and temperatures (7). The abundance of native Au in soils and placers is a function of relative concentration caused by chemical and mechanical weathering of rock hosting the primary mineralization, and by mechanical accumulation in fluvial environments rather than Au solubilization, biomineralization, and in situ growth under surface conditions (7). While this model explains the origin of some rare, large Au nuggets, it does not account for the majority of native Au in surface environments, which occurs as small secondary Au grains weighing less than 0.5 g. These are commonly <98 wt% pure, in contrast to large Au nuggets and primary Au that usually consist of a Au/Ag alloy (7). In many hydrothermal deposits, primary Au is present only as "invisible Au," i.e., in nanoparticulate (<100 nm) or lattice-bound forms within Fe-As sulfides (39); yet, secondary Au grains occur around such deposits (10). Therefore, secondary Au grains are coarser than primary Au (11), and display a wide range of morphologies including wire, dendritic, octahedral, porous, and sponge Au that are not commonly observed in source ores (40). These morphologies often consist of individual crystals or crystal aggregates with delicate shapes that would withstand the mechanical forces associated with fluvial transport, suggesting in situ formation (41).

To be available to organisms for biomineralization, Au needs to be mobile. Au(III) has a $5d^8$ electron configuration and establishes four coordinate, square planar complexes; the major ligands for Au(III) in nature are Cl^-, Br^-, and OH^- (30). In contrast, Au(I) is a "soft" metal center and forms both mononuclear and multinuclear compounds with a wide range of ligands. Au(I) has a $5d^{10}$ electronic configuration and in aqueous solution prefers linear complexes with two unidentate ligands; chloride and bisulfide complexes are most commonly invoked in natural environments (30, 42) although other S-, C-, and N-bearing ligands may play an important role in Au(I) speciation in surface waters, e.g., cyanide, amines/ammines, thiosulfate, and thiourea (30). Particularly in regions with oxidizing groundwater with high Cl^- contents found in arid and semiarid zones, soluble Au may occur as Au(III/I)-hydroxo-chloride-bromide-complexes (29, 43). Au concentrations in soil solution from auriferous soils can reach more than 100 parts-per-billion (ppb) (10) and are possibly even higher in solutions surrounding Au grains due to localized dissolution of Au. The Au concentrations detected in solution (up to 200 ppb) in microcosms amended with pure Au pellets (99.99 wt%) show that microbial activity led to a doubling of Au concentrations in solution, compared to the microcosms not amended with Au (10). Similar results were also obtained in microcosms with auriferous soils from semiarid and tropical zones in Australia (44). This suggests that Au is continuously mobilized on the surface of Au grains leading to highly toxic microenvironment. The presence of biofilms capable of catalyzing the biomineralization of secondary Au is thus the result of the toxicity exerted by Au-complexes on microbiota. Their toxicity in connection with their nonspecific uptake by different channels and transporters has forced organisms living on Au grains to strictly control metal-ion homeostasis and Au resistance (5). Our study has also shown that Au(III)-complexes are toxic to microorganisms at very low concentration: the MIC of Au(III) in *C.*

metallidurans CH34 is 2 μM (equivalent to 400 ppb Au in solution), and toxic effects to the organism start at ≈1/1,000 of the MIC (i.e., 0.4 ppb) (5). Thus, toxic effects to microorganisms are likely to occur in Au-rich soils, groundwater, and in particular in biofilms on Au grains, and having developed mechanisms to detoxify their cell environment, means a survival advantage for *C. metallidurans.*

Conclusions

We have shown that the biomineralization of particulate Au in *C. metallidurans* is the result of Au-regulated gene expression leading to the energy-dependent reductive precipitation of toxic Au-complexes. Hence, this research provides direct evidence that bacteria are actively involved in the biogeochemical cycling of rare and precious metals. Other precious metals, e.g., PGEs, share geochemical properties with Au (45). Like with Au, zones of secondary PGE enrichment occur in surface environments and were attributed to their solubilization, transport and precipitation (46). Sulfate-reducing bacteria and cyanobacteria have been shown to form Pt and Pd biominerals after amendment with Pt- and Pd-complexes (47, 48). Some authors also suggest that surface processes play a role in the formation of metallic Pt, Pd, Ru, Os, and Ir grains in placer deposits (49). This suggests that biogeochemical cycling of PGE is likely, and that multidisciplinary studies like the one presented here are pivotal in understanding these cycles. The discovery of active microbially driven biomineralization may lead to the development of technical applications, such as biosensor- (34, 35) and for ore processing technology. Likely, the Au-specific genetic responses identified may lead to the development of Au-specific biosensor technology enabling in situ Au measurements that could revolutionize the exploration for Au deposits and improve efficiency in Au extraction and hydrometallurgical processes.

Materials and Methods

Full Methods are available in *SI Materials and Methods*).

Viable, inactive, and dead *C. metallidurans* CH34 cultures were incubated in the presence of 50 μM Au(III)-complexes at pHs of 5.0 to 8.0 for 6 h and 144 h, and Au uptake was measured using ICP-MS. Thermodynamic data indicate that aqueous Au(III) in the experimental solutions existed as a negatively charged square planar complex, with mixed hydroxychloride complexes $[AuCl_x(OH)_{4-x}]^-$ dominating under between pH 5.0 and 8.0 (30). To assess the distribution and speciation of Au in individual cells amended with Au(III) synchrotron μXRF (with a focused beam size below 250 nm^2) and μXANES, data of individual cells were collected at two microprobe beam lines, i.e., 2-ID-D at the APS in Argonne (for *C. metallidurans* CH34 and *Desulfovibrio* sp.), and ID22NI at the ESRF in Grenoble, France (*C. metallidurans* CH34). This data were supplemented with TEM-EDS of ultra-thin sections of *C. metallidurans* cells containing Au nanoparticles, as well as SEM-EDS of natural biofilms on Au grains from the Prophet Gold Mine, Queensland, Australia. Transcriptome microarray experiments were conducted to assess the response of *C. metallidurans* CH34 to aqueous Au(III)-complexes and identify possible biochemical pathways for Au(III/I)-detoxification and Au(III/I)-speciation. Four Au(III) treatment conditions were chosen, i.e., 10, 50, and 100 μM, for 10 min, and 50 μM Au(III) for 30 min (*SI Materials and Methods* and Table S1).

ACKNOWLEDGMENTS. We thank the Advanced Photon Source (APS), the European Synchrotron Research Facility (ESRF), and the Stanford Synchrotron Radiation Laboratory (SSRL) for provision of beamtime; Barrick Gold and Newmont Gold for support; the Natural Sciences and Engineering Research Council Canada, which supported research at the University of Saskatchewan; P. Self, L. Waterhouse, and L. Green at Adelaide Microscopy; and J. Parson from Prophet Gold Mine for access and support. This work was supported by the Australian Research Council and Australian Synchrotron Research Funding Schemes.

1. Lowenstam HA (1981) Minerals formed by organisms. *Nature* 211:1126–1131.
2. Southam G, Saunders JA (2005) The geomicrobiology of ore deposits. *Econ Geol* 100:1067–1084.
3. Reith F, Dürr M, Welch S, Rogers SL (2008) in *Regolith Science*, eds Scott K, Pain CF (CSIRO Press, Melbourne, Australia), pp 127–159.
4. Reith F, Lengke MF, Falconer D, Craw D, Southam G (2007) Winogradski Review —The geomicrobiology of gold. *ISME J* 1:567–584.
5. Nies DH (1999) Microbial heavy metal resistance. *Appl Microbiol Biotechnol* 51:730–750.
6. Mergeay M, et al. (2003) *Ralstonia metallidurans*, a bacterium specifically adapted to toxic metals: Towards a catalogue of metal-responsive genes. *FEMS Microbiol Rev* 27:385–410.
7. Hough RM, Butt CRM, Reddy SM, Verrall M (2007) Gold nuggets: Supergene or hypogene? *Austr J Earth Sci* 54:959–964.
8. Clough DM, Craw D (1989) Authigenic gold-marcasite association—evidence for nugget growth by chemical accretion in fluvial gravels, Southland, New Zealand. *Econ Geol* 84:953–958.
9. Korobushkina ED, Karavaiko GI, Korobushkin IM (1983) in *Environmental Biogeochemistry, Ecology Bulletin 35*, ed Hallberg R (Publishing House of the Swedish Research Councils, Stockholm, Sweden), pp 325–333.
10. Reith F, McPhail DC (2006) Effect of resident microbiota on the solubilization of gold in soils from the Tomakin Park Gold Mine, New South Wales, Australia. *Geochim Cosmochim Acta* 70:1421–1438.
11. Mossman DJ, Reimer T, Durstling H (1999) The geochemistry of Witwatersrand-type gold deposits and the possible influence of ancient prokaryotic communities on gold dissolution and precipitation. *Geosci Can* 26:131–140.
12. Checa SK, Espariz M, Audero ME, Botta PE, Spinelli SV, Soncini FC (2007) Bacterial sensing of and resistance to gold salts. *Mol Microbiol* 63:1307–1318.
13. Reith F, Rogers SL, McPhail DC, Webb D (2006) Biomineralization of gold: Biofilms on bacterioform gold. *Science* 313:333–336.
14. Nakajima A (2003) Accumulation of gold by microorganisms. *WJ Microbiol Biotechn* 19:369–374.
15. Mack C, Wilhelmi B, Duncan JR, Burgess JE (2007) Biosorption of precious metals. *Biotechn Adv* 25:264–271.
16. Edwards PP, Thomas JM (2007) Gold in a metallic divided state—from Faraday to present-day nanoscience. *Angew Chem Int Ed* 46:5480–5486.
17. Rouf MA (1964) Spectrochemical analysis of inorganic elements in bacteria. *J Bacteriol* 6:1545–1549.
18. Norris V, et al. (1996) Calcium signalling in bacteria. *J Bacteriol* 13:3677–3682.
19. Lengke M, et al. (2006) Mechanisms of gold bioaccumulation by filamentous cyanobacteria from gold(III)-chloride complex. *Environ Sci Technol* 40:6304–6309.
20. Lengke MF, Southam G (2006) Bioaccumulation of gold by sulfate-reducing bacteria cultured in the presence of gold(I)-thiosulfate complex. *Geochim Cosmochim Acta* 70:3646–3661.
21. Wackett LP, Dodge AG, Ellis LBM (2004) Microbial genomics and the periodic table. *Appl Environ Microbiol* 70:647–655.
22. Bentley R, Chasteen TG (2002) Microbial methylation of metalloids: Arsenic, antimony, and bismuth. *Microbiol Molecul Biol Rev* 66:250–271.
23. Anderson GK (1982) The organic chemistry of gold. *Adv Organometal Chem* 20:39–114.
24. Panmanee W, Vattanaviboon P, Poole LB, Mongkolsuk S (2006) Novel organic hydroperoxide-sensing and responding mechanisms for OhrR, a major bacterial sensor and regulator of organic hydroperoxide stress. *J Bacteriol* 188:1389–1395.
25. Monchy S, et al. (2006) Transcriptomic and proteomic analyses of the pMOL30-encoded copper resistance in *Cupriavidus metallidurans* strain CH34. *Microbiol* 152:1765–1776.
26. Stoyanov JV, Brown NL (2003) The *Escherichia coli* copper-responsive copA promoter is activated by gold. *J Biolog Chem* 278:1407–1410.
27. Jian X, et al. (2009) Highly sensitive and selective gold(I) recognition by a metalloregulator in *Ralstonia metallidurans. J Chem Soc* 131:10869–10871.
28. Monchy S, et al. (2007) Plasmids pMOL28 and pMOL30 of *Cupriavidus metallidurans* are specialized in the maximal viable response to heavy metals. *J Bacteriol* 189:7417–7425.
29. Vanysek P (1990–1991) in *CRC Handbook of Chemistry and Physics*, ed Lide DR, (CRC Press, Boca Raton, FL), 71st Ed, pp 8–16.
30. Usher A, McPhail DC, Brugger J (2009) A spectrophotometric study of aqueous Au(III) halide-hydroxide complexes at 25–80 °C. *Geochim Cosmochim Acta* 73:3359–3380.
31. Konishi Y, et al. (2006) Intracellular recovery of gold by microbial reduction of $AuCl_4^-$ ions using the anaerobic bacterium *Shewanella algae. Hydrometallurgy* 81:24–29.
32. Gardea-Torresdey JL, et al. (2002) XAS investigations into the mechanism(s) of Au(III) binding and reduction by alfalfa biomass. *Microchem J* 71:193–204.
33. Carney CK, Harry SR, Sewell SL, Wright DW (2007) Detoxification biominerals. *Top Curr Chem* 270:155–185.
34. Ledrich M-L, et al. (2005) Precipitation of silver-thiosulfate complex and immobilisation of silver by *Cupriavidus metallidurans* CH34. *Biometals* 18:643–650.
35. Corbisier P (1997) Bacterial metal-lux biosensors for a rapid determination of the heavy metal bioavailability and toxicity in solid samples. *Res Microbiol* 148:534–536.
36. Corbisier P, et al. (1999) Whole cell- and protein-based biosensors for the detection of bioavailable heavy metals in environmental samples. *Anal Chim Acta* 387:235–244.
37. Pontel LB, et al. (2007) GolS controls the response to gold by hierarchical induction of *Salmonella*-specific genes that include a CBE efflux-coding operon. *Mol Microbiol* 66:814–825.
38. Grosse C, Friedrich S, Nies DH (2007) Contribution of extracytoplasmic function sigma factors to transition metal homeostasis in *Cupriavidus metallidurans* strain CH34. *J Mol Microbiol Biotechnol* 12:227–240.
39. Helmann JD (2002) The extracytoplasmic (ECF) sigma factors. *Adv Microbiol Physiol* 46:47–110.
40. Cook NJ, Chryssoulis SL (1990) Concentration of ''invisible gold'' in the common sulfides. *Can Mineral* 28:1–16.
41. Hough RM, et al. (2008) Naturally occurring gold nanoparticles and nanoplates. *Geology* 336:571–574.
42. Stefansson A, Seward TM (2004) Gold(I) complexing in aqueous sulphide solutions to 500 degrees C at 500 bar. *Geochim Cosmochim Acta* 68:4121–4143.
43. Krauskopf KB (1951) The solubility of gold. *Econ Geol* 46:858–870.
44. Reith F, McPhail DC (2007) Microbial influences on solubilisation and mobility of gold and arsenic in regolith samples from two gold mines in semi-arid and tropical Australia. *Geochim Cosmochim Acta* 71:1183–1196.
45. Rauch S, Morrison GM (2008) Environmental relevance of the platinum-group elements. *Elements* 4:259–263.
46. Gray DJ, Schorin KH, Butt CRM (1995) Mineral associations of platinum and palladium in lateritic regolith, Ora Banda Sill, Western Australia. *J Geoch Explor* 57:245–255.
47. Lengke MF, Fleet M, Southam G (2006) Synthesis of platinum nanoparticles by reaction of filamentous cyanobacteria with platinum(IV)-chloride complex. *Langmuir* 22:7318–7323.
48. Rashamuse KJ, Whitely CG (2007) Bioreduction of Pt (IV) from aqueous solution using sulphate-reducing bacteria. *Appl Microbiol Biotechnol* 75:1429–1435.
49. Cabral AR, Galbiatti HF, Kwitko-Ribeiro R, Lehmann B (2008) Platinum enrichment at low temperatures and related microstructures, with examples of hongshiite (PtCu) and empirical 'Pt_2HgSe_3' from Itabira, Minas Gerais, Brazil. *Terra Nova* 1:32–37.